



# Behavior of Eurofer97 reduced activation martensitic steel upon heating and continuous cooling

A. Danón \*, A. Alamo

*Commissariat à l'Énergie Atomique, Centre d'Études Nucléaires de Saclay, 91191 Gif-sur-Yvette, France*

## Abstract

The phase transformation behavior of the Eurofer97 steel (Fe9Cr1WVTa) has been investigated. The transformation temperatures upon heating and cooling were determined by dilatometry for different rates in the range 0.0028–100 °C/s. The prior austenitic grain size of Eurofer97, measured as a function of the austenitization temperature, does not change appreciably up to 1050 °C and then increases with increasing austenite temperature from 1050 up to 1200 °C. Continuous cooling transformation diagrams were determined for the austenitization temperatures of 980, 1060 and 1140 °C. They show a well-known form with two main phase fields, martensite and ferrite. Values of the critical cooling rates and ferrite start temperatures depend on the austenitization temperature. After thermal cycles samples were further characterized by optical microscopy, scanning electron microscopy and thermoelectric power measurements.

© 2002 Elsevier Science B.V. All rights reserved.

## 1. Introduction

Martensitic steels of the CrWVTa type present an attractive combination of different properties required for applications to internal components of fusion reactors: high swelling resistance, adequate mechanical and thermophysical properties as well as the potential of a lower induced activity after irradiation [1,2]. To optimize the behavior of these low activation materials, it is necessary to have a good insight into their physical metallurgy.

Some CrWVTa low activation alloys were previously studied [3]. The present work deals with phase transformations occurring during heating and continuous cooling of the Eurofer97 steel, which is the first reduced activation heat of the CrWVTa type manufactured at the industrial scale in Europe. The temperatures of austenite occurrence by varying the heating rate and the evolution of the austenite mean grain size as a function of the annealing temperature was investigated. The

effects of prior austenite grain size on the kinetics of continuous cooling transformations (CCTs) were considered as well.

## 2. Material

Eurofer97 steel was manufactured by Böhler (Austria) as plates in the normalized and tempered condition, i.e. austenitized at 980 °C for 31 min and tempered at 760 °C for 90 min. The heat identification code is E83698. The chemical composition of Eurofer97 – as determined by our own chemical analysis – is shown in Table 1.

The LA12LC steel, a nearly Ta-free (100 ppm) alloy with chemical composition similar to Eurofer97 (see Table 1) was used to compare the austenite grain size evolution. LA12LC was supplied by UK AEA Culham (UK); it was austenitized at 1030 °C for 40 min and tempered at 750 °C for 60 min with a final cold-working of 10%.

## 3. Experimental

The anisothermal phase transformations of the alloy Eurofer97 were studied by dilatometric techniques for

\* Corresponding author. Present address: Université de Paris Sud–Faculté des Sciences d'Orsay, Bât 410, 91405 Orsay cedex, France. Tel.: +33-1 691 54789; fax: +33-1 691 57833.

E-mail address: [ariel.danon@lpces.u-psud.fr](mailto:ariel.danon@lpces.u-psud.fr) (A. Danón).

Table 1  
Chemical composition of the Eurofer97 and LA12LC steels (wt%)

Alloy	C	Si	Mn	Cr	V	W	N	Ta	Ni
Eurofer97	0.12	0.03	0.48	8.96	0.18	1.04	0.022	0.15	0.06
LA12LC	0.089	0.03	1.13	8.92	0.30	0.73	0.035	0.01	–

different heating and cooling rates. In all cases, the initial metallurgical state of the samples was the normalised-tempered condition.

For the determinations of transformation temperatures from ferrite/martensite to austenite, samples were heated up to 1135 °C at rates ranging from 0.08 to 100 °C/s. The on-cooling, anisothermal phase transformations from the austenite phase field were studied after annealing for 30 min at 980, 1060 and 1140 °C. Cooling rates ranged from 8 to 300 °C/h. CCT diagrams were established for each selected austenitization temperature. The accuracy of the measured phase transformation temperatures for on-heating and on-cooling experiments was  $\pm 10$  °C.

The austenite grain size measurements were performed by image analysis after austenitization of samples in the range 1000–1200 °C for 30 min. To reveal the austenite grain boundaries, a special heat treatment was used to induce a preferential carbide precipitation during isothermal transformation into (ferrite + carbides) as described in Ref. [4].

Thermoelectric power (TEP) and Vickers hardness measurements were performed for samples transformed by continuous cooling. Samples were further examined by optical and scanning electron microscopy.

## 4. Results and discussion

### 4.1. Austenite grain size measurements

Fig. 1 displays the evolution of the austenite mean grain size with the annealing temperature for the Eurofer97 and LA12LC steels. Up to 1050 °C, the austenite grain size of Eurofer97 is almost constant and an important grain growth takes place beyond 1050 °C. The LA12LC Ta-free steel exhibits a continuous growth in the range 1030–1140 °C, and grain sizes systematically higher than Eurofer97 for the same austenitization conditions.

Thus, the Ta-containing steel Eurofer97 displays more refined grain sizes than the Ta-free steel, as was already shown for other low activation materials [5].

### 4.2. On-heating and on-cooling phase transformations

Fig. 2 shows the austenite start ( $A_s$ ) and austenite finish ( $A_f$ ) temperatures taken from dilatometric measurements as a function of the heating rate. The values  $A_{10}$ ,  $A_{50}$  and  $A_{90}$  (temperatures to reach 10%, 50% and

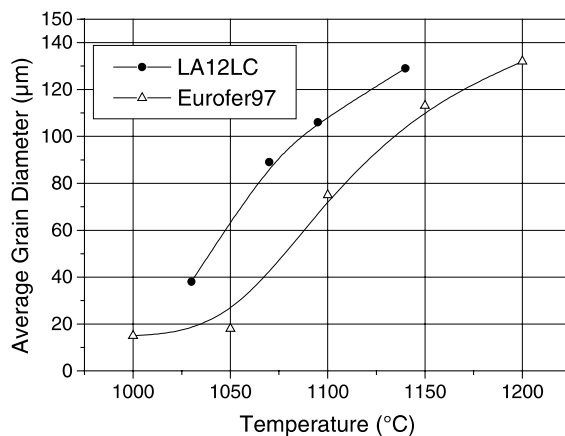


Fig. 1. Average austenitic grain size as a function of the austenitization temperature for Eurofer97 and LA12LC steels.

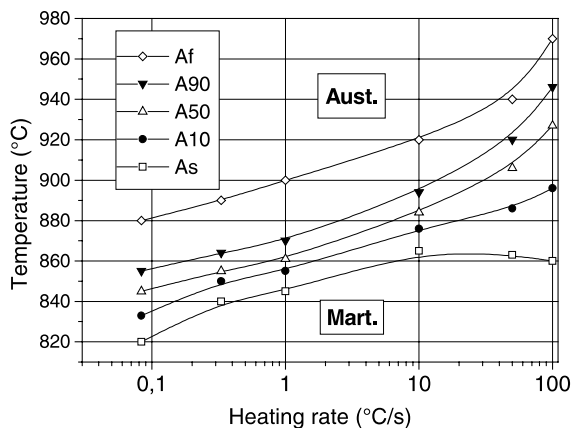


Fig. 2. On-heating transformation temperatures of Eurofer97 steel.

90% of austenite fraction, respectively) are also plotted. An increase of the transformation temperatures with heating rate is in general observed.

As expected, the CCT diagram of Eurofer97 showed two main phase fields, martensitic and ferritic, with no evidence of a bainitic transformation. The critical cooling rates (CCR), i.e.  $R_m$ , the minimum rate to obtain a full transformation of austenite into martensite and  $R_f$ , the maximum rate to obtain a full transformation of austenite into ferrite, were determined from metallographic observations and dilatometric curves.

The CCT diagram for the austenitization temperature of 980 °C is presented in Fig. 3.  $M_s$ ,  $M_f$ ,  $F_s$  and  $F_f$

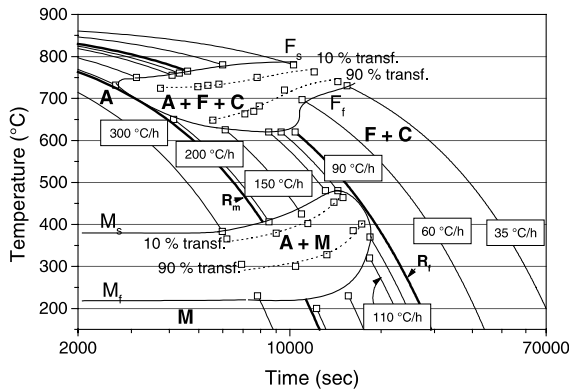


Fig. 3. CCT diagram obtained after austenitization at 980 °C for 30 min. A: austenite, M: martensite, F: ferrite, C: carbides.

indicate the temperature values for martensite and ferrite transformation start and finish, respectively. Higher austenitization temperatures stabilise the austenitic field and thus CCT diagrams showed a shift of the ferritic domain to lower values of CCR as shown in Table 2. Similar results have been previously reported, both for the reduced activation CrWVTa alloys [5] and for conventional martensitic steels of the 9Cr1Mo type [6].

On the other hand, the austenitization temperature has only a slight influence on the as-quenched martensite hardness and  $M_s$  values as shown in Table 2.

#### 4.3. Evolution of the $F_s$ and $M_s$ temperatures in the biphased field

The  $F_s$  temperature and the temperature to form 10% ferrite  $F_{10\%}$  decreased with increasing cooling rate in the biphased domain for each austenitization condition (see Fig. 3). In addition, the  $F_s$  temperature decreases – as shown in Fig. 4 – with increasing austenitization temperature.

For cooling rates of about 30 °C/h, an important decrease of  $F_s$  is obtained after raising the austenitization temperature from 1060 to 1140 °C. This behavior could be associated with the important increment of austenite mean grain size  $d_\gamma$  beyond 1050 °C. According to [7],  $F_s$  depends on the density of ferrite nucleation sites, that is, the austenite grain boundaries, edges and corners, which is, in turn, proportional to  $d_\gamma^{-1}$ ,  $d_\gamma^{-2}$  and

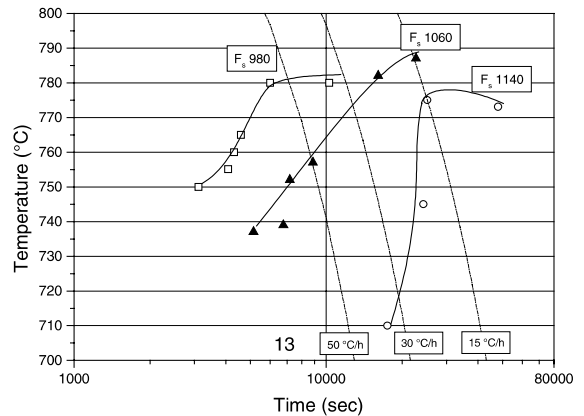


Fig. 4. Ferrite start temperature  $F_s$  as a function of the cooling rate and the austenitization temperature.

$d_\gamma^{-3}$ , respectively. In this way, larger austenitic grain sizes will result in a lower density of ferrite nucleation sites, which would produce, in turn, a decrease in the  $F_s$  temperature. An identical correlation between austenitization temperature and ferrite start temperature has been shown for the continuous cooling of microalloyed steels [8] and for the transformation behavior of C–Mn–Ni weld metal [9].

The  $M_s$  and  $M_f$  temperatures increase with decreasing cooling rates in the biphased domain (Fig. 3). The  $M_s$  increase reached approximately 80 °C, for each austenitization condition. Among the factors that control the  $M_s$  temperature, the interstitial carbon content could be the main one. The observed behavior indicates a corresponding decrease in the amount of carbon in solid solution in the austenite not transformed into ferrite. Hence, a carbon impoverishment in austenite should occur simultaneously with the nucleation and growth of ferrite. This fact can only be explained by a significant carbide precipitation.

On the other hand, no definite dependence of the  $M_s$  temperature with respect to the austenitization temperature could be established for the investigated ranges of cooling rates.

#### 4.4. Microstructure

The austenitization temperature affects markedly the proportions of the microstructural constituents in the

Table 2  
CCR values obtained for each austenitization temperature

Austenite temp. (°C)	$R_m$ (°C/h)	$R_f$ (°C/h)	$HV5_{\text{mart.}}$	$HV5_{\text{ferr.}}$	$M_s$ (°C)
980	210	90	408	139	383
1060	150	15	400	151	387
1140	50	10	393	125	400

The  $M_s$  and  $HV5_{\text{mart.}}$  values correspond to a cooling rate of 300 °C/h.

biphased field. The fraction of martensite phase (roughly estimated from dilatometric curves) increases with the austenitization temperature. Fig. 5(a) and (b) show the microstructure obtained after cooling from 1140 °C at two typical cooling rates  $R$  corresponding respectively to (a)  $R \leq R_m$  (martensitic matrix showing the start of ferrite + carbide precipitation) and (b)  $R \approx R_f$  (fully ferritic condition). The austenite  $\rightarrow$  ferrite transformation is initiated at austenite grain corners and boundaries and the ferrite nucleation is always accompanied by carbide precipitation, as shown in Fig. 5(a).

Various types of carbide precipitation morphologies developed during cooling: pearlitic-like, precipitation on ferrite grain boundaries and bulk precipitation. The pearlitic-like morphology becomes dominant for the lower cooling rates (Fig. 5(b)), but a coarse intragranular precipitation and precipitation along ferrite grain boundaries are also observed.

#### 4.5. TEP measurements

Fig. 6 shows TEP measurements as a function of the cooling rate for each austenitization temperature. This magnitude is strongly dependent on the amount of interstitials in solid solution in the sample [10]. Thus, the fully ferritic matrix displayed a much lower TEP value than the fully martensitic one, the corresponding interstitial (C + N) content assumed to be about 200 and 1300 ppm respectively. On the other hand, TEP values for fully martensitic samples cooled at 300 °C/h were almost identical for the samples austenitized from 980 to 1140 °C, which would mean that the free interstitial content is not significantly altered in this temperature range.

TEP values of biphased samples decreased from the martensite value to the ferrite one on going from high to

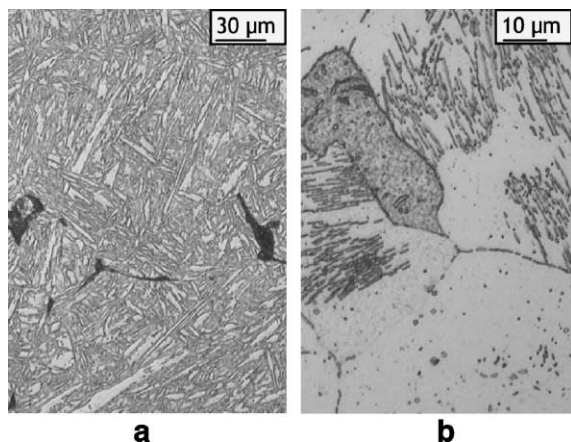


Fig. 5. Microstructures obtained after cooling from 1140 °C at  $R \leq R_m$  (a) and  $R \approx R_f$  (b).

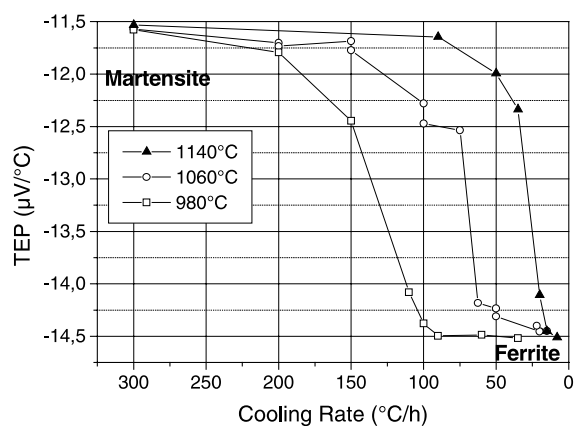


Fig. 6. TEP evolution as a function of the cooling rate.

low cooling rates, for each austenitization condition. As discussed in [11], this diminution is not only the result of the increasing ferrite fraction but also of the carbon impoverishment of the non-transformed austenite during cooling. This carbon impoverishment is evidenced by the already mentioned ascending behavior of the  $M_s$  temperature, and suggests that the carbon solubility in austenite is considerably lowered during cooling.

The variation of TEP for the interstitial content change  $\Delta[C + N]_y$ , and the fraction 'y' of ferrite transformed under cooling could be described by the following relationship:

$$TEP_y = (1 - y)(TEP_M - \beta\Delta[C + N]_y) + yTEP_x, \quad (1)$$

where  $TEP_M$  and  $TEP_x$  are the characteristic TEP values for the fully martensitic and fully ferritic matrix respectively. The coefficient  $\beta$  accounts for the relationship, assumed to be linear as shown in [11], between the variation in TEP and the free interstitial content values. From previous TEP measurements carried out on fully martensitic samples of different FeCrWVTa steels a value of  $\beta \approx 15 \mu V/(K \text{ wt}\%)$  was determined [11]. In our case, a rough estimation of  $\beta$  by linear interpolation between the  $TEP_M$  and  $TEP_x$  values (considering a ferrite interstitial content of 200 ppm) gives  $\beta \approx 25 \mu V/(K \text{ wt}\%)$ . According to expression (1), the estimated decrease of the interstitial content in the non-transformed austenite is about 850 ppm for a ferrite fraction of 80%. This figure indicates that the remaining interstitial content in solid solution in austenite could be as low as 400–450 ppm.

## 5. Conclusions

On-heating and on-cooling phase transformations of the Eurofer97 steel were studied. The effect of austeni-

tization treatments on the phase transformation behavior was investigated as well.

The prior austenitic grain size of Eurofer97 does not change significantly with temperature up to 1050 °C and then increases with the austenitization temperature from 1050 up to 1200 °C.

On-heating martensite to austenite transformation starts at 820–860 °C and finishes at 880–970 °C, depending on the heating rate (0.1–100 °C/s).

CCT diagrams were established for the austenitization temperatures of 980, 1060 and 1140 °C. Three types of microstructures were found at room temperature according to the cooling rate: ferritic, martensitic or biphased martensitic–ferritic. The CCR and ferrite start temperatures depend on prior austenite grain size. The martensite start temperature  $M_s$  increases with decreasing cooling rate for biphased samples.

Microstructural observations showed a variety of carbide precipitation morphologies, the pearlitic-like being the dominant one for the low cooling rates. TEP values display a pronounced decrease with cooling rate for all of the austenitization conditions, which could be related to the increment in the ferrite phase fraction and the austenite impoverishment in carbon during cooling. This impoverishment is evidenced by the observed increment in  $M_s$  values.

## Acknowledgements

Special thanks are given to F. Barcelo for her technical assistance in grain size determinations by image analysis.

## References

- [1] R.L. Klueh, JOM 44 (4) (1992) 20.
- [2] F. Abe, T. Noda, M. Okada, J. Nucl. Mater. 195 (1992) 51.
- [3] A. Alamo, J.C. Brachet, A. Castaing, C. Foucher, F. Barcelo, Final Report LAM3 Contract, Euratom/CEA Fusion Association, 1996.
- [4] F. Barcelo, J.C. Brachet, Rev. Metall. Cah. Inf. Tech. 91 (2) (1994) 255.
- [5] A. Alamo, J.C. Brachet, A. Castaing, C. Lepoittevin, F. Barcelo, J. Nucl. Mater. 258–263 (1998) 1228.
- [6] J.C. Brachet, A. Alamo, Mém. Et. Sci. Rev. Mét. 87 (1990) 33.
- [7] M. Militzer, R. Pandi, E.B. Hawbolt, Metall. Mater. Trans. 27A (1996) 1547.
- [8] Th.A. Kop, P.G.W. Remijn, J. Sietsma, S. van der Zwaag, Mater. Sci. Forum 284–286 (1998) 193.
- [9] R.A. Farrar, Z. Zhang, S.R. Bannister, G.S. Barritte, J. Mater. Sci. 28 (1993) 1385.
- [10] R. Borrelly, D. Benkirat, Acta Metall. 33 (1985) 855.
- [11] J.C. Brachet, J. Phys. IV (France) 5 (12) (1995) 339.